Int. J. Heat Mass Transfer. Vol. 27, No. 10, pp. 1801–1812, 1984
Printed in Great Britain

0017–9310/84 $3.00 + 0.00
Pergamon Press Ltd.

Recirculating mixed convection flow for energy extraction

C. K. CHA* and Y. JALURIA

Department of Mechanical and Aerospace Engineering, Rutgers University, New Brunswick, NJ 08903, U.S.A.

(*Received* 8 *April* 1983 *and in revised form* 3 *January* 1984)

Abstract—Energy may be extracted from the sensible heat stored in a body of fluid by means of a recirculating flow. A numerical study of the time-dependent, two-dimensional, laminar, convective flow that arises is carried out. The hot fluid is withdrawn at the top and the cold fluid discharged at the bottom of the storage region to preserve the thermal stratification. The nature of the flow is found to be very strongly affected by the buoyancy and the flow configuration. Numerical results are presented over a wide range of governing parameters, that arise from the inflow conditions, flow configuration and the heat transfer mechanisms at the boundaries.

INTRODUCTION

IN THE past few years, considerable research effort has been directed at energy storage systems, which are necessary for solar energy applications because of the intermittent availability of solar radiation. Various studies have considered energy storage in rock beds, phase change materials and in enclosed water bodies [1]. Hot water storage has been studied extensively, particularly for space and water heating [2–4]. Salt-gradient solar ponds have also been studied because of their considerable promise for collection and long-term storage of solar energy [5, 6]. Most of these studies were largely directed at the design, analysis and operation of the energy storage system. As a consequence, considerable information exists on the effect of various physical variables, relevant to a given storage system, on its performance, particularly for long-term storage.

A problem which is of considerable importance in hot water storage systems is that of energy extraction. Effort has been directed at internal heat exchangers and also at recirculating flows with external heat exchangers, the latter being of greater interest and promise due to the much greater ease in maintenance and larger thermal efficiency [5–7]. However, a recirculating flow with an external heat exchanger generally results in much greater flow velocities, which may disrupt the thermal stratification in a hot water storage system and also disturb the nonconvective zone of a salt-gradient solar pond [8, 9]. The flow may also short circuit between the inflow and the outflow channels, resulting in a much lower extracted fluid temperature. These considerations make it important to determine the flow field in the storage tank and study its dependence on the physical variables of the problem, such as flow configuration, inflow and outflow conditions, thermal conditions at the boundaries and geometry of the water body. Of particular interest would be the transient behavior of the outflow temperature and the temperature field that arises [10, 11].

The present study considers the mixed convection flow that arises in an enclosed water body due to the extraction of thermal energy by means of a recirculating fluid flow. The outflow of the hot fluid from the storage region is taken at the top and the inflow at the bottom, considering two configurations resulting from locating the inflow and the outflow on the same or opposite ends of the region. The temperature and flow fields are studied numerically for a laminar, two-dimensional (2-D) flow over wide ranges of the governing parameters. Since the transient and periodic processes, with periodic heat input, are of interest in these energy storage systems, the study is mainly concerned with the transient effects that arise. The steady-state situation, in many cases, is the trivial attainment of the ambient temperature by the storage fluid. Since this problem is of particular concern in solar ponds, the study also considers the boundary conditions relevant to that circumstance. A matter of considerable interest in this study is the spread of the flow in the storage region, since a greater spread implies energy extraction from a greater portion of the storage region. This is of particular importance when the inflow and the outflow are located at the same end of the water body.

It is found that the flow in the storage region is strongly dependent on the locations of the inflow and the outflow channels. The effect of buoyancy is found to be very significant and the velocity and temperature fields are strongly affected by the inlet conditions, given in terms of the parameter Gr/Re^2. A stable thermal stratification is found to arise in an initially isothermal heated water region due to energy extraction which results in the discharge of colder fluid at the bottom of the storage region. The effect of the flow on the stability of the nonconvective zone in a solar pond is also considered. The dependence of the temperature of the extracted fluid on the flow configuration and on the governing parameters is studied in detail. The

* Present address: Foster Wheeler Development Corp., Livingston, NJ 07039, U.S.A.

NOMENCLATURE

d height of inflow and outflow channels [m]
g magnitude of gravitational acceleration [m s^{-2}]
Gr Grashof number, $g\beta(T_0-T_i)d^3/\nu^2$
H depth of storage region [m]
k thermal conductivity of fluid [W m^{-1} K^{-1}]
L length of storage region [m]
p local pressure [N m^{-2}]
Pr Prandtl number, ν/α
q_H heat flux input into the storage region at the bottom surface [W m^{-2}]
q_0 heat flux lost at the top surface [W m^{-2}]
Q_H dimensionless heat gain parameter, $q_H d/k(T_0-T_i)$
Q_0 dimensionless heat loss parameter, $q_0 d/k(T_0-T_i)$
Re Reynolds number, $U_0 d/\nu$
T local temperature [K]
T_i initial uniform temperature in storage region [K]
T_0 inlet fluid temperature [K]
u horizontal velocity component [m s^{-1}]
U dimensionless horizontal velocity, u/U_0
U_0 inlet flow velocity [m s^{-1}]
v vertical velocity component [m s^{-1}]
V dimensionless vertical velocity, v/U_0
x horizontal coordinate distance [m]
X dimensionless horizontal coordinate distance, x/d
y vertical coordinate distance [m]
Y dimensionless vertical coordinate distance, y/d.

Greek symbols
α thermal diffusivity of the fluid [m^2 s^{-1}]
β coefficient of thermal expansion of the fluid [K^{-1}]
θ dimensionless temperature, $(T-T_i)/(T_0-T_i)$
ν kinematic viscosity [m^2 s^{-1}]
ρ fluid density [kg m^{-3}]
τ' physical time [s]
τ dimensionless time, $\tau'/(d/U_0)$
ψ' streamfunction [m^2 s^{-1}]
ψ dimensionless streamfunction, $\psi'/U_0 d$
ω' vorticity [s^{-1}]
ω dimensionless vorticity, $\omega'/(U_0/d)$.

underlying physical processes are discussed in terms of the results obtained and the relevance of these results to the design of a physical energy extraction system is outlined. Several interesting, important and, sometimes, surprising results are obtained. A comparison with results obtained in earlier studies indicated a reasonably good agreement.

ANALYSIS

The coordinate system for the two flow configurations considered is shown in Fig. 1. The cold water from the energy extraction process in an external heat exchanger flows into the storage region at the bottom and the hot water from the tank is withdrawn at the top. The two circumstances corresponding to the opposite-end and the same-end configurations relate to two extreme cases of maximum and minimum horizontal distance between the inflow and outflow channels. Since the latter is more economical, in terms of tubing and pumping costs, it is more attractive. However, it is important to determine the flow penetration into the water body for effective heat extraction. Since the inflowing water is colder and, thus, heavier, it is expected to flow along the floor a greater distance, before recirculating towards the outflow, than if there were no buoyancy effect. Similarly, for the other configuration, the flow spread in the storage zone is an important consideration.

The governing equations for the laminar, 2-D unsteady flow under consideration are obtained, with the usual Boussinesq approximations, as [12, 13]

$$\frac{\partial u}{\partial x}+\frac{\partial v}{\partial y}=0 \tag{1}$$

$$\frac{\partial u}{\partial \tau'}+u\frac{\partial u}{\partial x}+v\frac{\partial u}{\partial y}=-\frac{1}{\rho}\frac{\partial p}{\partial x}+\nu\left(\frac{\partial^2 u}{\partial x^2}+\frac{\partial^2 u}{\partial y^2}\right) \tag{2}$$

$$\frac{\partial v}{\partial \tau'}+u\frac{\partial v}{\partial x}+v\frac{\partial v}{\partial y}=-\frac{1}{\rho}\frac{\partial p}{\partial y}+\nu\left(\frac{\partial^2 v}{\partial x^2}+\frac{\partial^2 v}{\partial y^2}\right)-g\beta(T-T_i) \tag{3}$$

$$\frac{\partial T}{\partial \tau'}+u\frac{\partial T}{\partial x}+v\frac{\partial T}{\partial y}=\alpha\left(\frac{\partial^2 T}{\partial x^2}+\frac{\partial^2 T}{\partial y^2}\right) \tag{4}$$

where the equations are coupled through the buoyancy term in the y-momentum equation. This study assumes laminar flow, which applies for small flow rates, as characterized by the inlet Reynolds number Re. For turbulent flow, a suitable turbulence model may be employed. In this study, an eddy viscosity model was also employed to obtain the velocity and temperature fields. Though the corresponding results are not presented here, the basic features and trends observed for laminar flow were found to be quite similar to those for turbulent flow.

The initial and boundary conditions for the above

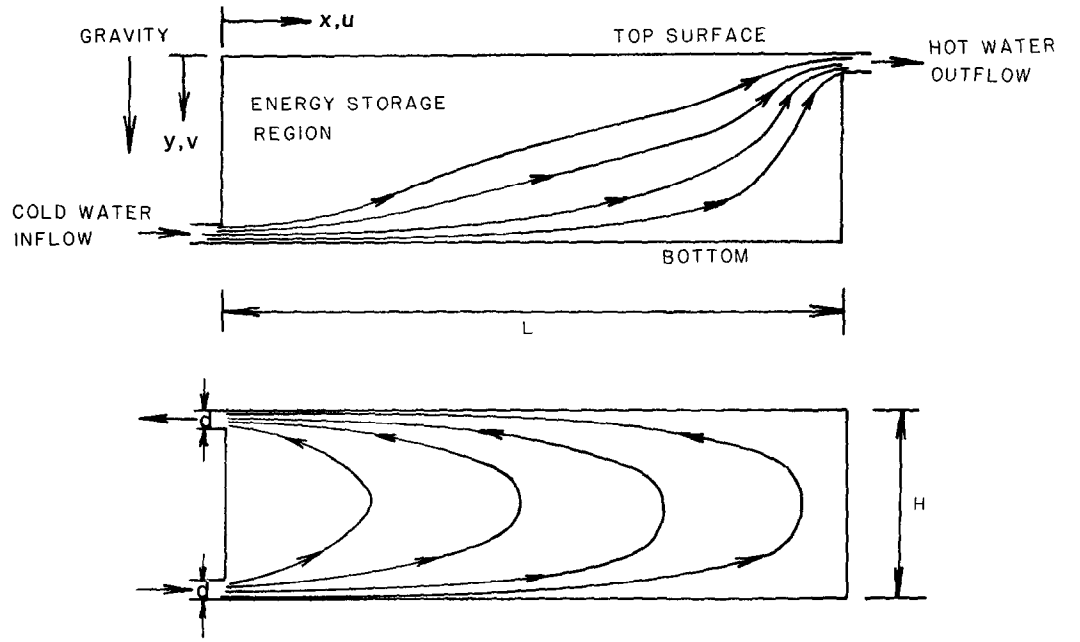

FIG. 1. Flow configurations and the coordinate system.

equations may now be considered. The inflow and outflow channels were taken to be of the same height d and the storage zone to be of height H and length L. At the inflow and outflow, a uniform velocity U_0 was assumed and no-slip conditions were employed at the bottom and at the side walls. For a solar pond, the upper surface is a zero-shear condition, with slip at the interface with the nonconvective zone [8]. As a result, both zero-shear and no-slip conditions were considered at the upper horizontal boundary. Heat transfer at the top and bottom boundaries was considered and the side walls were taken as adiabatic. These conditions may, thus, be written for the same-end configuration, with no-shear at the upper boundary, as

$$\text{at} \quad \tau' = 0; \quad u = v = T - T_i = 0 \quad \text{for} \quad 0 \leqslant x \leqslant L, \quad 0 \leqslant y \leqslant H$$

$$\text{for} \quad \tau' > 0; \quad u = v = \frac{\partial T}{\partial x} \quad \text{for} \quad x = 0, \quad d \leqslant y \leqslant (H-d)$$

$$\text{and for } x = L, \quad 0 \leqslant y \leqslant H \tag{5}$$

$$\frac{\partial u}{\partial y} = v = 0, \quad k\frac{\partial T}{\partial y} = q_0, \quad \text{at} \quad y = 0$$

$$u = v = 0, \quad k\frac{\partial T}{\partial y} = q_H, \quad \text{at} \quad y = H$$

$$u = -U_0, \quad v = 0, \quad T = T_0, \quad \text{at} \quad x = 0, \quad 0 < y < d$$

$$u = U_0, \quad v = 0, \quad \frac{\partial T}{\partial x} = 0, \quad \text{at} \quad x = 0, \quad (H-d) < y < H$$

where q_0 is the heat flux lost at the top surface and q_H that gained by the water body at the bottom. Similarly, the conditions for the other flow configuration of Fig. 1 may be written.

The above system of equations is solved with the corresponding boundary conditions, by employing the conservative vorticity–streamfunction formulation [13–15]. Employing d as the characteristic length dimension to nondimensionless x and y and U_0 the velocity to nondimensionalize u and v, the dimensionless streamfunction, vorticity and time are given by

$$\psi = \psi'/U_0 d, \quad \omega = \omega'/(U_0/d), \quad \tau = \tau'(d/U_0) \tag{6}$$

where $u = \partial\psi'/\partial y$ and $v = -\partial\psi'/\partial x$. The temperature is nondimensionalized as

$$\theta = \frac{T - T_i}{T_0 - T_i} \tag{7}$$

which gives the initial nondimensional temperature as zero and the temperature at the inflow as 1.0. With the above nondimensionalization, the governing vorticity, streamfunction and temperature equations are obtained, in terms of the Reynolds, Grashof and Prandtl numbers, Re, Gr and Pr, as

$$\frac{D\omega}{D\tau} = \frac{1}{Re}\nabla^2\omega - \frac{Gr}{Re^2}\frac{\partial\theta}{\partial X} \tag{8}$$

$$\omega = -\nabla^2\psi \tag{9}$$

$$\frac{D\theta}{D\tau} = \frac{1}{Re\,Pr}\nabla^2\theta. \tag{10}$$

The boundary conditions yield H/d and L/d as additional parameters, along with the heat transfer

parameters Q_0 and Q_H, at the two horizontal boundaries, where

$$Q_0 = q_0 d/k(T_0 - T_i) \quad \text{and} \quad Q_H = q_H d/k(T_0 - T_i). \tag{11}$$

The boundary conditions may be written in terms of ψ and ω by employing the relationships between them and the velocity components [13–15].

The governing equations were solved numerically, employing finite-difference methods. The alternating direction implicit (ADI) method of Peaceman and Rachford [16] was employed for the vorticity and energy equations, the streamfunction equation being solved by successive over-relaxation or cyclic reduction [14]. A 21×21 or a 41×41 grid was employed for the results presented here, with a time step of the order of 0.05 and a convergence criterion of around 10^{-4} on the streamfunction at each time step. An effect of less than 1–2% on ψ was observed when the grid spacing was halved. Similarly, the time step and the convergence criteria were varied to ensure a negligible dependence of the results on the values chosen.

The study considers wide ranges of the governing parameters Re, Gr, L/H, Q_0 and Q_H for a Prandtl number of 3.5 which applies for typical water temperatures encountered in such a storage system. Other values were also considered and a weak dependence of the thermal and flow fields on the Prandtl number was found in the range 3.0–7.0. The Reynolds number was varied up to 1000 for laminar flow in the inlet channel. However, the jet may undergo transition to turbulence after discharge into the water body at these high values of Re. The mixed convection parameter Gr/Re^2 was varied up to around 1.0. The aspect ratio L/H was varied from 1.0 to 100.0 and the ratio H/d was kept at 10.0, in the presented results, for convenience, since it was found to have a small effect on the observed trends. Because of the complexity of the numerical problem under consideration, fairly large computing times, with typical values of around 100 min, were needed on a VAX 11/780 computer system. Though various other boundary conditions were considered in this study [17], the results presented here are for the no-shear, slip, condition on the flow at the upper boundary. This condition closely approximates the case of solar ponds and of other hot water storage systems with a free surface.

Before presenting the numerical results, a few comments may be made regarding the assumptions employed. For the range of temperatures generally encountered in such energy storage systems, the constant property assumption, with the Boussinesq approximation, is satisfactory. However, property variation may easily be incorporated in the numerical scheme if the dependence of the properties on the temperature is known and if larger temperature variations are of interest. The 2-D flow assumption is made since it is desirable to spread out the flow horizontally, over the entire storage region, and to keep the flow velocities low, particularly in a solar pond where large velocities may lead to the destabilization of the gradient zone. In practice, the flow will tend to be three-dimensional (3-D) near the inlet and the outlet. But if several inlet and outlet ports are positioned linearly, the flow is expected to be 2-D in much of the flow region. It must also be noted that, in solar ponds, the salt concentration is essentially uniform in the storage zone and, therefore, only the thermal effects need to be considered in the flow.

The heat loss at the upper boundary is treated in terms of a constant value of Q_0. In actual practice, it will vary with temperature of the storage zone and, thus, with time. This effect can be considered if large energy extraction times are employed. For large values of Q_H, i.e. heating from below, turbulence may result from the unstable stratification that arises. Though results are presented here only for $Q_H = 0$, nonzero values were also considered [17] and a fairly localized effect on the thermal field was observed for small values of Q_H. For large values, turbulence will have to be considered. However, very little experimental work has been done on this problem and the inputs needed for a satisfactory modeling of turbulent flow are not available. We shall now present some of the typical results obtained in this study, indicating several interesting and important features relevant to heat extraction.

RESULTS AND DISCUSSION

The results presented here concern the two flow configurations of Fig. 1 and the time-dependent temperature and velocity fields, obtained numerically, are discussed. Figure 2 shows the streamlines for the end-to-end configuration at $Re = 100, L/H = 10.0, Q_0 = 0.2$ and $Q_H = 0$, for three values of the buoyancy parameter Gr/Re^2. The results are shown at dimensionless time $\tau = 800$, which corresponds to an essentially quasi-steady situation. The flow is established very rapidly following the start of energy extraction. However, the thermal effect spreads outwards from the inlet very gradually due to diffusion and convection. As this effect penetrates towards the outflow, the flow field also changes gradually due to the buoyancy coupling. In the absence of buoyancy, the flow field attains steady state in a very short time [15]. Therefore, the flow undergoes a slowly-varying transient due to the buoyancy. In the absence of heat loss or gain at the boundaries, the steady state is attained when the entire water body attains the inlet temperature. However, such a steady state is of little interest in energy extraction, which would generally be continued only until the outlet temperature indicates a substantial decrease from the initial value. Most of the results shown here are, therefore, well into the transient regime and correspond to a slowly-varying flow field.

Several interesting features are seen in Fig. 2. The flow is obviously strongly dependent on the parameter Gr/Re^2. In the absence of buoyancy, the flow field in an enclosure with rigid boundaries is expected to be symmetric about the midplane, an approximate

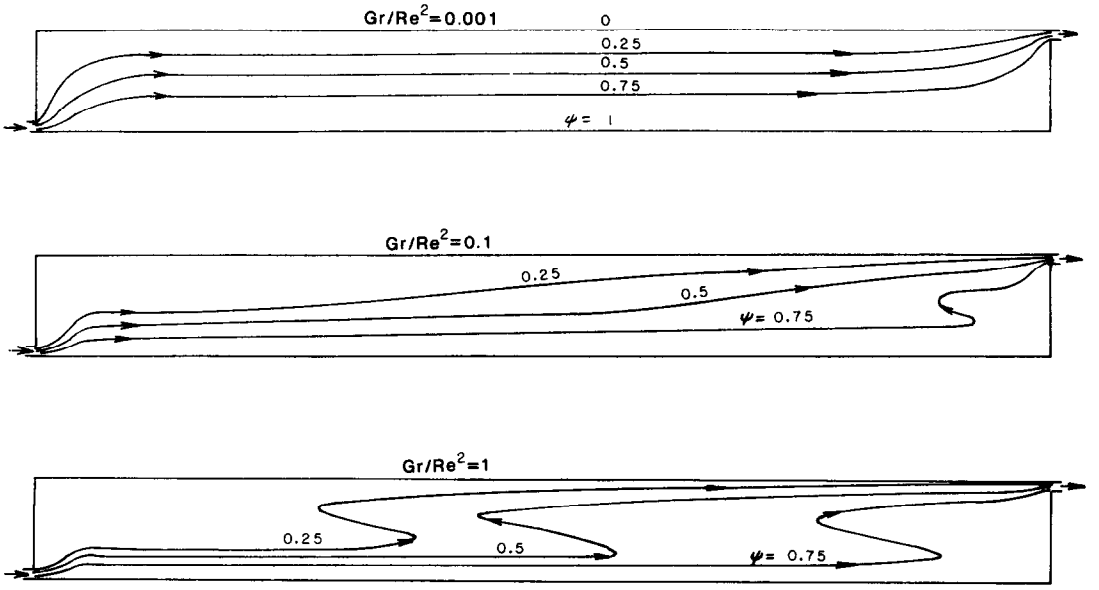

FIG. 2. Calculated streamlines at $Re = 100, L/H = 10.0, Q_0 = 0.2, Q_H = 0$ and $\tau = 800$ for various values of the parameter Gr/Re^2.

behavior being observed at the lowest value of Gr/Re^2. However, as this parameter increases, the flow indicates a considerable change. It is seen that at $Gr/Re^2 = 1.0$, the incoming flow tends to stay near the floor over a much larger distance than that observed at the lower values. This is expected from the relatively greater negative buoyancy of the inflowing fluid and is a trend which is similar to that in heated surface jets [18]. This flow must rise up towards the outflow due to continuity and the associated pressure effect. However, as the colder fluid rises, it encounters hotter and, thus, more buoyant fluid. This results in a horizontal deflection of the flow, followed by an ultimate flow towards the outlet. This flow reversal, seen clearly at $Gr/Re^2 = 1.0$ and to a much smaller extent at $Gr/Re^2 = 0.1$, is, therefore, the result of the interaction between the buoyancy and pressure forces. Due to heat loss at the surface, the local temperature in the upper region decreases and, consequently, so does the buoyancy defect, which results in an earlier turnaround of the flow than otherwise. At even larger values of Gr/Re^2, more flow reversals, in several horizontal layers, are

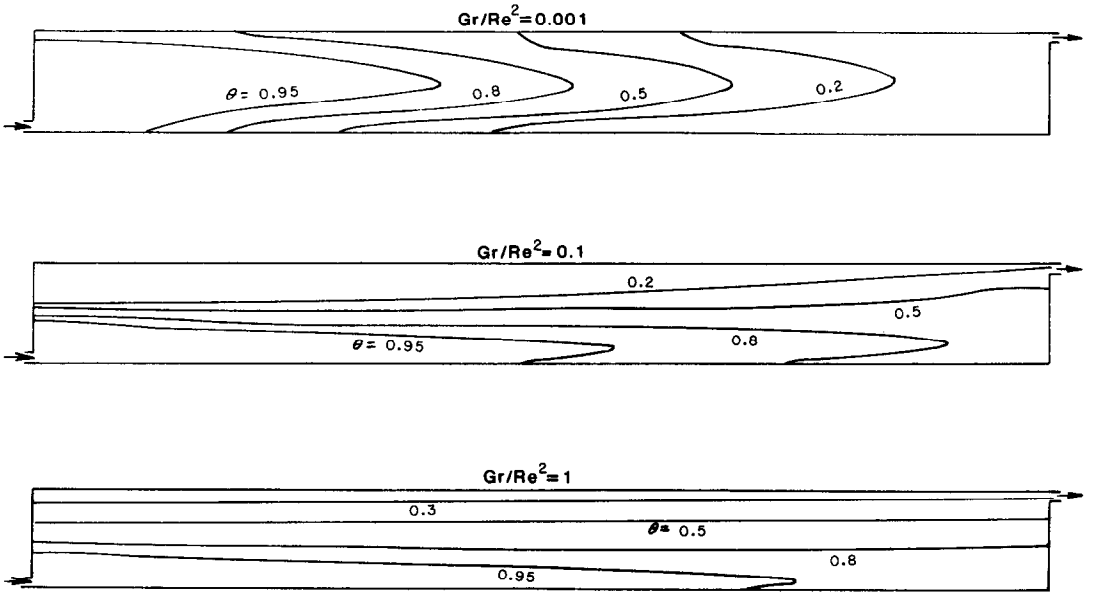

FIG. 3. Isotherms for the end-to-end configuration at $Re = 100$, $L/H = 10.0$, $Q_0 = 0.2$, $Q_H = 0$ and $\tau = 700$.

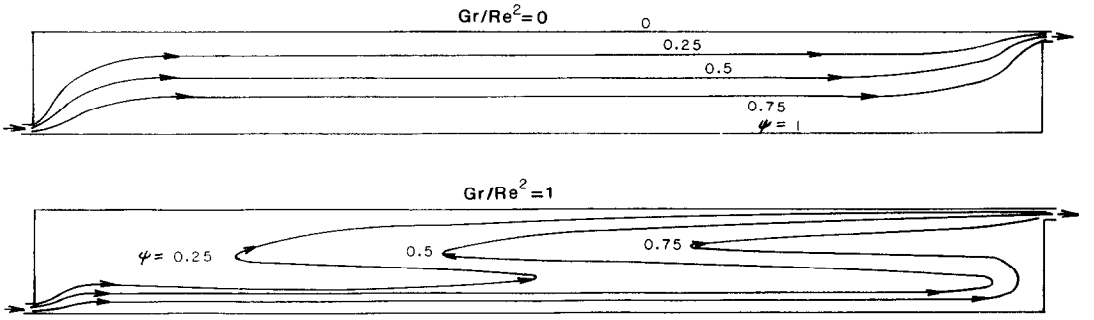

FIG. 4. Streamlines at $Re = 1000$, $L/H = 10.0$, $Q_0 = 0.2$, $Q_H = 0$ and $\tau = 760$ for $Gr/Re^2 = 0$ and 1.0.

expected. The flow field observed at $Gr/Re^2 = 1.0$ also indicates the generation of stably stratified layers because of reduction in vertical convective mixing.

The temperature field corresponding to the above flow is shown in Fig. 3. At $Gr/Re^2 = 10^{-3}$, the penetration of the thermal effect outwards from the inflow is seen to be quite symmetric about the horizontal midplane. At $Gr/Re^2 = 1.0$, the storage region is found to be strongly stratified, with almost horizontal layers arising from the flow field, discussed earlier. The surface is cooler than the region below it because of the imposed heat loss condition there. The corresponding temperature profiles are discussed later. However, it is evident from Fig. 3 that the thermal field is also strongly dependent on the parameter Gr/Re^2 and a strong stably stratified circumstance is found to arise at large values.

Figure 4 shows the flow field at $Re = 1000$ and $\tau = 760$. The results are shown for the zero buoyancy effect case, $Gr/Re^2 = 0$, and at $Gr/Re^2 = 1.0$. The former circumstance shows an essentially symmetric flow at steady state, which is attained well before the time at which results are shown. At the larger Gr/Re^2, flow reversal similar to that observed in Fig. 2, is obtained. The flow stays near the floor over a larger distance in this case, as compared to the corresponding flow at $Re = 100$, and the flow region adjacent to the floor is narrower. A larger Re implies a larger inflow momentum, which would be expected to penetrate further, but the flow reversals are also stronger because of the larger velocity level. The narrowing of the flow region near the floor and also near the top surface is similar to the corresponding effect in boundary layer flows with increasing Re. Due to the strong horizontal flow and weak vertical flow, stably stratified fluid layers again arise in this case.

The flow field that arises in the same-end configuration is shown in Fig. 5 at $Re = 1000$, $L/H = 10.0$, $Q_0 = 0.2$ and $Q_H = 0$ for three values of $Gr/Re^2 = 0$, 0.1 and 1.0. The first streamline plot is obtained for the zero buoyancy case of $Gr/Re^2 = 0$. The flow recirculates from the inflow to the outflow, with a very small penetration into the storage region. The inflowing fluid has a horizontal momentum that drives

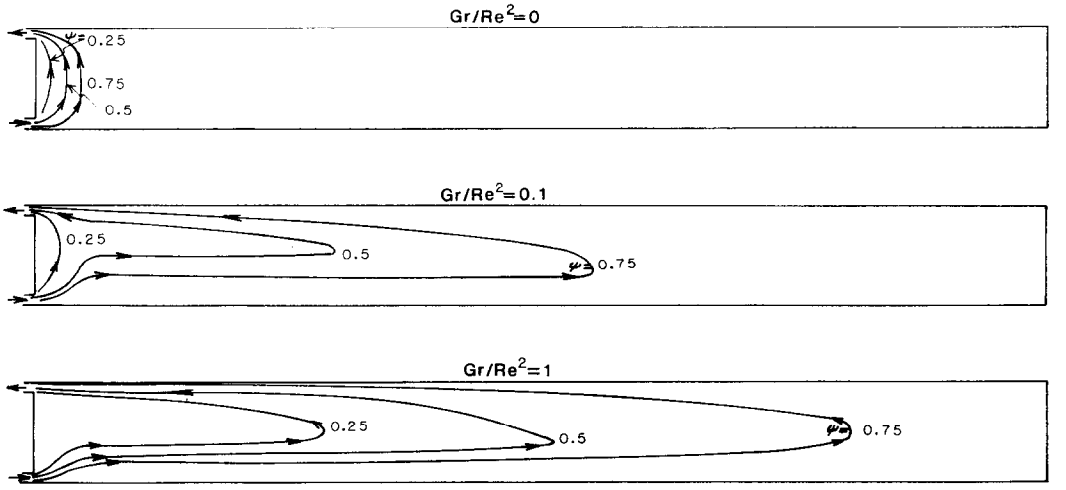

FIG. 5. Streamlines for the same-end configuration at $Re = 1000$, $L/H = 10.0$, $Q_0 = 0.2$, $Q_H = 0$ and $\tau = 800$ for various values of Gr/Re^2.

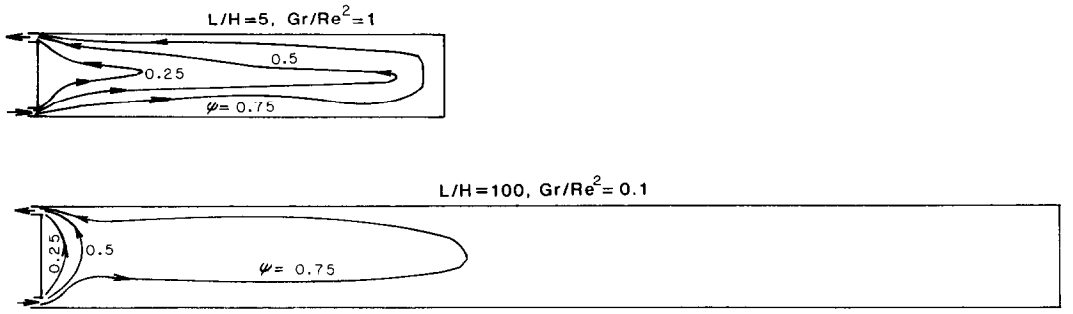

FIG. 6. Effect of aspect ratio on the flow for the same-end configuration at $Re = 1000$, $Q_0 = Q_H = 0$ and $\tau = 2000$.

it across the storage region. The outflow, on the other hand, generates a pressure difference due to continuity and this pressure effect causes the fluid to rise towards the outlet. A consequence of the flow at $Gr/Re^2 = 0$ is a large, essentially undisturbed, region of fluid, from which energy extraction occurs only by natural convection, the main flow being restricted to a region near one end. This is obviously not a desirable feature in energy extraction. With increasing Gr/Re^2, the flow penetration increases, since the heavier inflowing fluid tends to stay near the floor for a larger distance due to negative buoyancy. At $Gr/Re^2 = 1.0$, the flow penetrates almost to the far end and better energy extraction characteristics are, therefore, expected. The inflow conditions, specified in terms of U_0, T_0 and d, may be varied to obtain the largest possible penetration, or the length L of the storage region may be chosen suitably to extract energy from the entire region. These aspects are considered again later in this section. These results are shown at $\tau = 800$, which is also in the quasi-steady domain of the transient convective flow.

The effect of the aspect ratio L/H at $Re = 1000$ for the same-end configuration is shown in Fig. 6. No heat loss or gain is considered at the boundaries and the flows shown are again in the gradually-varying flow field region of the energy extraction process. The flow penetration at $L/H = 5$ and $Gr/Re^2 = 1.0$ is found to be quite satisfactory, since the entire region is subjected to convective transport. At $L/H = 100$ and $Gr/Re^2 = 0.1$, only a small portion of the region is involved. A comparison with the corresponding results for $L/H = 10$ in Fig. 5 indicates a considerable extension of the $\psi = 0.75$ streamline, though the flow near the inflow–outflow end is not strongly affected. At this value of Gr/Re^2, the far end does not affect the flow very much, as seen in Fig. 5, and, therefore, a larger length would not affect the main flow near the inflow very strongly. However, a weak flow persists to large distances from the near end at larger values of the aspect ratio.

The isotherms for this flow configuration at $Re = 100$, $L/H = 10.0$, $Q_0 = 0.2$ and $Q_H = 0$ are shown in Fig. 7 for three values of the parameter Gr/Re^2 at $\tau = 600$. At the highest value of Gr/Re^2, the thermal field is found to spread out over the entire region and a

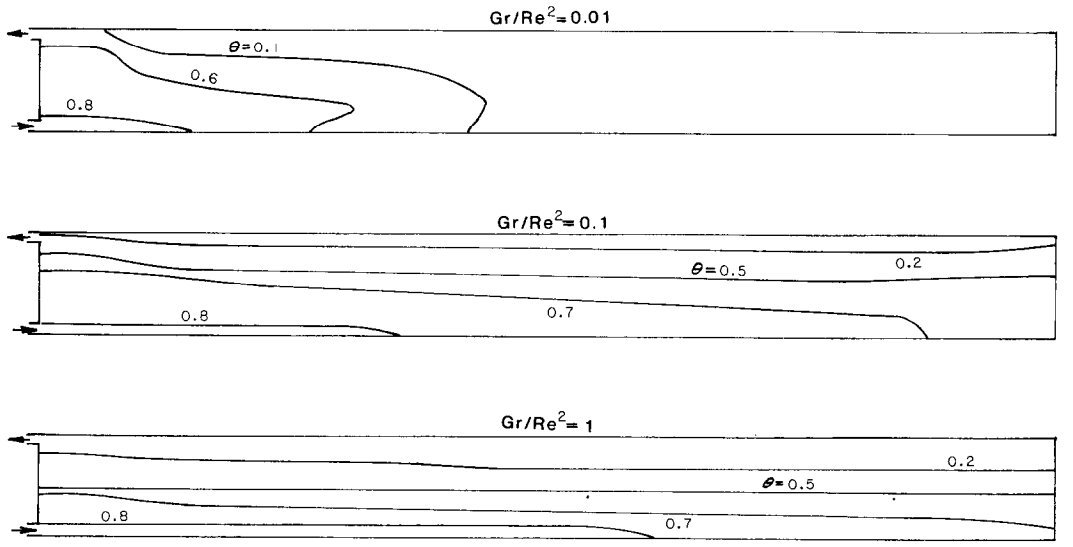

FIG. 7. Isotherms at $Re = 100$, $L/H = 10$, $Q_0 = 0.2$, $Q_H = 0$ and $\tau = 600$ for various values of Gr/Re^2.

stably stratified circumstance is found to arise. At low values of Gr/Re^2, a much smaller penetration occurs and much of the storage region stays undisturbed for a long time following the start of energy extraction.

The corresponding velocity and temperature profiles at the midplane for the two flow configurations are shown in Figs. 8 and 9. The flow reversal in the end-to-end configuration and the recirculation in the same-end configuration are clearly seen, the effects being accentuated as Gr/Re^2 increases. The storage region is found to be stably stratified, except near the boundaries if heat loss or gain is present. For the end-to-end configuration the thermal effect is found to be concentrated in the midsection at low Gr/Re^2, with higher temperatures both above and below. This is expected from the streamlines and isotherms seen earlier. As Gr/Re^2 increases, the flow stays near the floor and lower temperatures arise at the bottom and the temperature increases towards the top surface. Recall that a higher value of θ implies a lower temperature, with $\theta = 1.0$ at the inlet, and a lower value indicates a higher temperature, with $\theta = 0$ at the start, $\tau = 0$.

It is seen from Figs. 8 and 9 that at large values of Gr/Re^2, large flow velocities arise at the top surface. For a salt-gradient solar pond, this boundary is the interface between the storage zone and the nonconvective gradient layer. It is important to determine the effect of the recirculating flow on the stability of the nonconvective zone. The Richardson number Ri based on the velocity at the surface and typical density profiles in the gradient zone [5, 8] was determined considering various depths over which the disturbance occurs. Since for $Ri > 0.85$, negligible entrainment into the flow occurs from a stratified region [18], the depth to which appreciable disturbance arises may be determined. Even for the outflow located at the top, as considered here, the disturbance to the gradient zone was found to be restricted to a very small region near the interface. If the outflow is moved a few centimetres away from the interface, the disturbance to the gradient zone was found to decrease sharply. Thus, this system may be suitably designed for use in energy extraction from solar ponds.

The variation of the outlet temperature θ_b with time

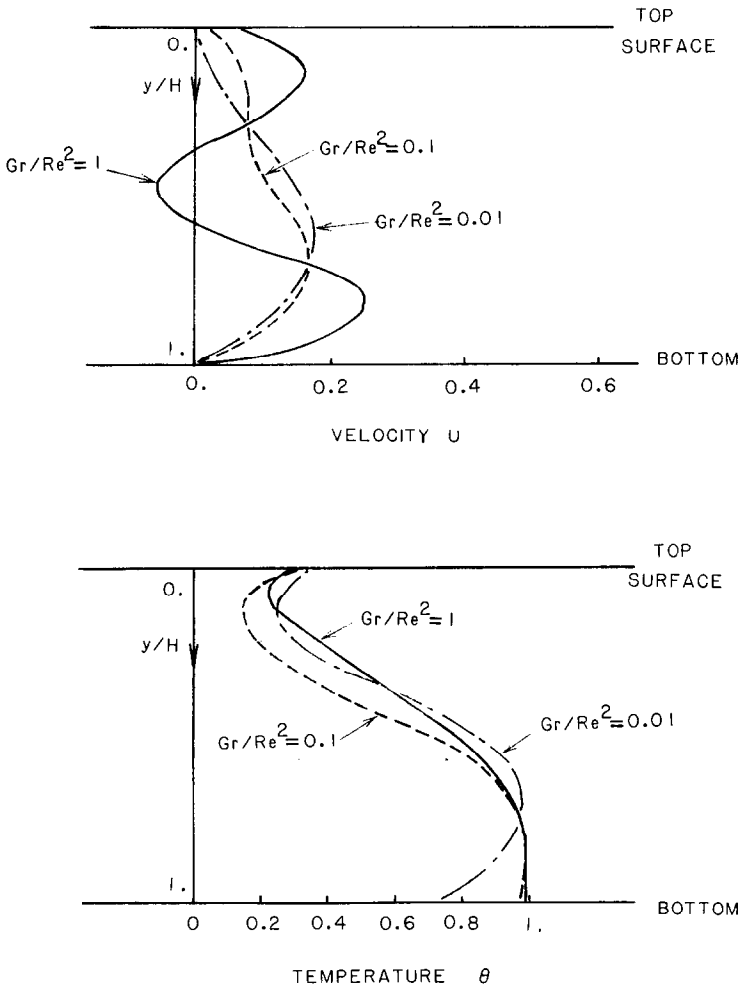

FIG. 8. Velocity and temperature profiles at the midplane for the end-to-end configuration at $Re = 100$, $L/H = 10.0$, $Q_0 = 0.2$, $Q_H = 0$ and $\tau = 700$.

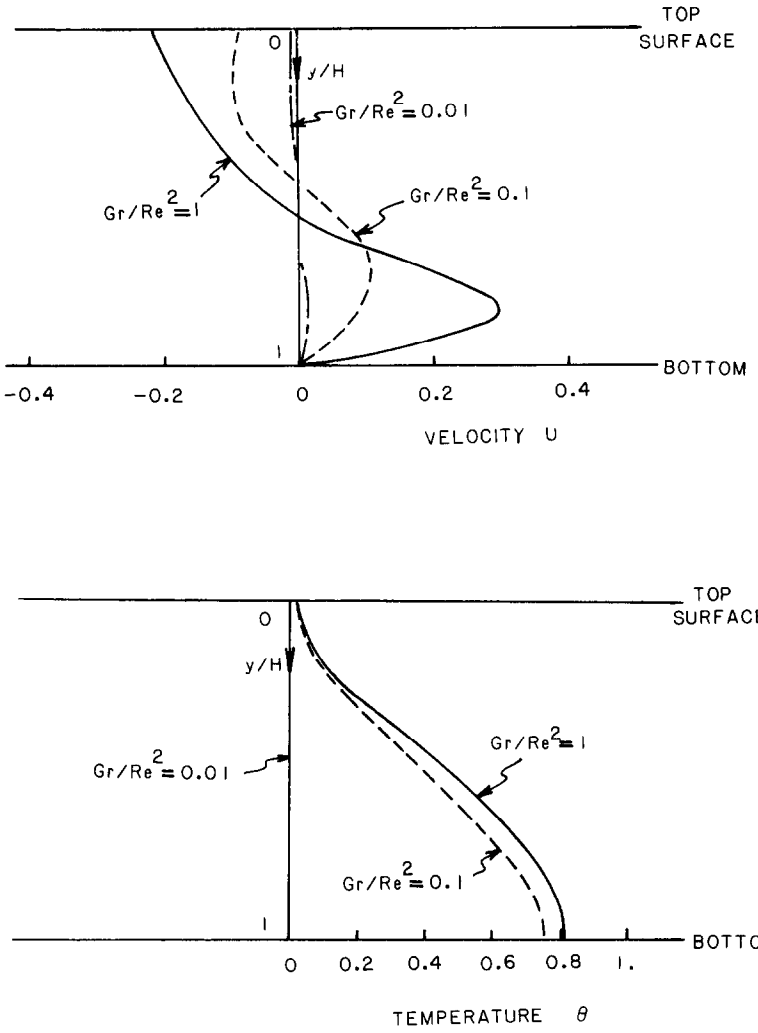

FIG. 9. Velocity and temperature profiles at the midplane for the same-end configuration at $Re = 100$, $L/H = 10.0$, $Q_0 = Q_H = 0$ and $\tau = 600$.

for the two configurations is shown in Fig. 10 at $Re = 1000, Gr/Re^2 = 1.0$ and $0.001, L/H = 10.0, Q_0 = 0.2$ and $Q_H = 0$. It is interesting to note the tremendous difference between the two at the lower value of Gr/Re^2. The inflowing cold water recirculates to the outflow very rapidly for the same-end configuration, causing the outlet temperature to start dropping almost immediately. This effect may be reduced by increasing H and Gr/Re^2. The case shown does not involve heat input at the bottom. If there is heating from below, it tends to heat up the inflowing fluid and, thus, reduce the negative buoyancy effect. The initial decrease in θ_b was found to be more gradual if Re and Q_H are smaller, as expected from the effect these have on the flow recirculation. The end-to-end configuration is, on the other hand, found to be excellent, since the outlet temperature is held essentially constant for a fairly long time. However, in view of the economic attractiveness of the same-end configuration, it is obviously desirable to employ a combination of the two extreme configurations so as to minimize cold water recirculation to the outflow, while keeping the distance between the inflow and the outflow at a minimum. A proper choice of inlet conditions will also help in making the same-end configuration more effective for energy extraction. This is clearly seen from the results at $Gr/Re^2 = 1.0$ for which the trends for the two configurations are quite close.

A similar consideration is indicated in Fig. 11, where the penetration, in terms of the $\psi = 0.9$ streamline, is given as a function of Gr/Re^2 at two Reynolds number values, for the same-end configuration. As seen before, penetration increases with an increase in Gr/Re^2 and with a decrease in Re. Therefore, the appropriate values of H and L may be chosen for given inflow conditions, or vice versa, for effective heat extraction. Several other results were obtained along these lines and the above discussion indicates the general trends observed.

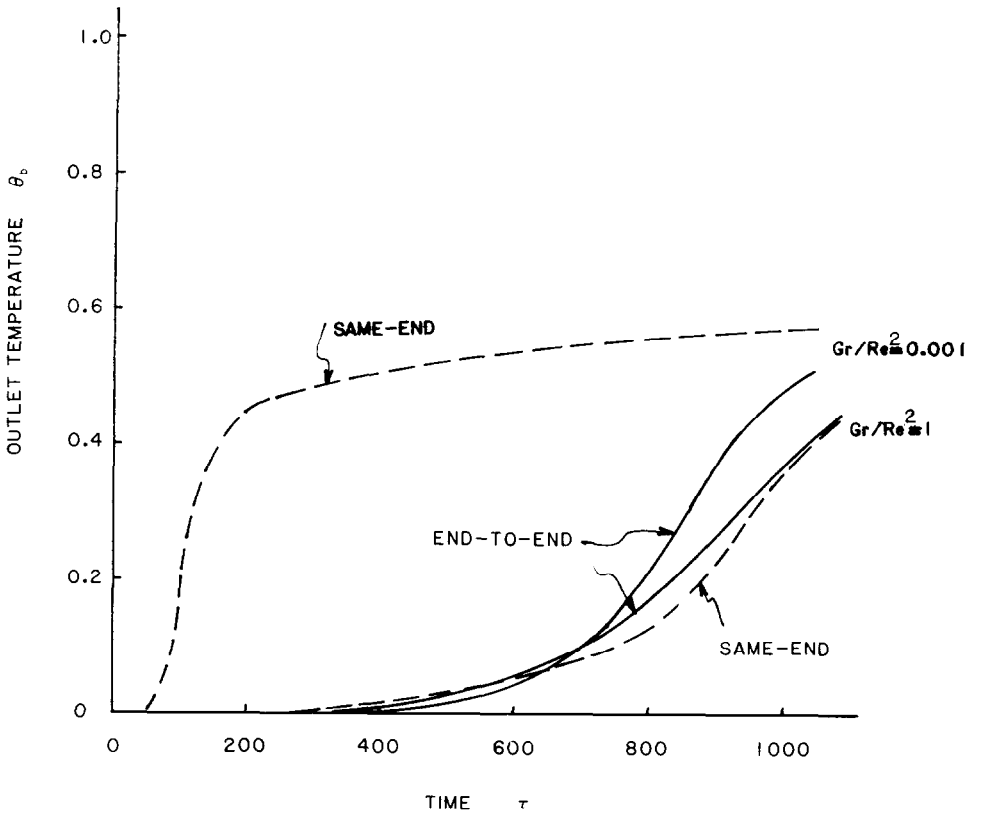

FIG. 10. Variation of the outlet dimensionless temperature θ_b with time for the two configurations at $Re = 1000$, $Gr/Re^2 = 1.0$ and 0.001, $L/H = 10$, $Q_0 = 0.2$ and $Q_H = 0$.

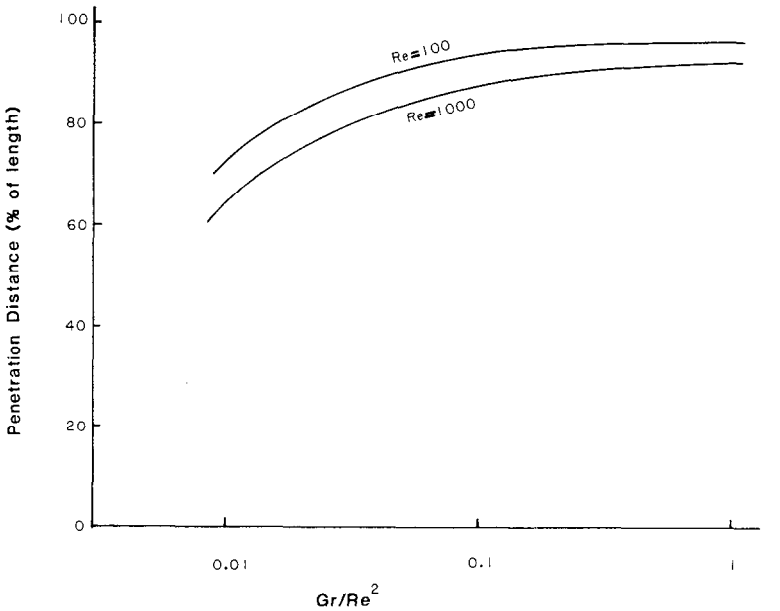

FIG. 11. Dependence of the flow penetration, in terms of percentage of length, for the same-end configuration on the parameters Re and Gr/Re^2 at $\tau = 800$, with $Q_0 = 0.2$, $Q_H = 0$ and $L/H = 10.0$.

CONCLUSIONS

Energy extraction from a hot water storage system, by means of a recirculating flow, has been studied numerically to determine the time-dependent flow and temperature fields that arise. Two flow configurations, corresponding to the extreme cases of inlet and outlet channels located on the same side and on the opposite sides of the storage zone, are considered, with hot water extraction at the top and cold water inflow at the bottom. Of particular interest was the dependence of the mixed convection flow in the enclosed fluid region on the inlet conditions, characterized by the Reynolds and Gashof numbers, and on the flow configuration. It was found that the flow is strongly dependent on the mixed convection parameter Gr/Re^2, which determines the relative buoyancy effect. At increasing values of this parameter, the flow is found to penetrate further into the storage zone in the same-end configuration and to result in flow reversals for the other configuration. The fluid region is found to be strongly stratified, with a weaker vertical convective mixing, at larger values of Gr/Re^2.

Another important consideration in the study is related to the temperature of the extracted fluid at the outlet. The outflow fluid temperature is determined as a function of time. For the same-end configuration, the outflow temperature is found to decrease soon after the onset of the flow for small Gr/Re^2, whereas for the end-to-end configuration, this temperature is held essentially constant over a much larger period of time, indicating the more effective energy extraction in the latter case. This behavior is also seen in terms of the flow spread and penetration in the storage region and the consequent convective mixing. The dependence of the flow and temperature fields on the various governing parameters, that arise from the inlet and boundary conditions, is studied in detail, to guide the choice of the physical variables in an actual system for effective energy extraction from the entire storage region. The study considers various boundary conditions, for velocity and for temperature, that apply for hot water storage systems, particularly solar ponds. For the simulation of solar ponds, a heat input at the bottom, a heat loss at the top surface and a no-shear boundary condition at the top surface are assumed and several results are presented for this circumstance. Various other cases are studied and the observed flow is considered in terms of the underlying physical processes. A comparison with similar earlier studies indicated a general agreement of the observed trends.

Acknowledgements—The authors acknowledge the support provided by the Department of Mechanical and Aerospace Engineering, Rurgers University, for this work and the several discussions with F. Zangrando at the Solar Energy Research Institute, Colorado, on this problem.

REFERENCES

1. F. Kreith and J. F. Kreider, *Principles of Solar Engineering*. Hemisphere, Washington, DC (1978).
2. Z. Lavan and J. Thompson, Experimental study of thermally stratified hot water storage tanks, *Solar Energy* **19**, 519–524 (1977).
3. A. Cabelli, Storage tanks—a numerical experiment, *Solar Energy* **19**, 45–54 (1977).
4. Y. Jaluria and S. K. Gupta, Decay of thermal stratification in a water body for solar energy storage, *Solar Energy* **28**, 137–143 (1982).
5. C. E. Nielsen, Nonconvective salt-gradient solar ponds, in *Solar Energy Handbook* (edited by W. C. Dickinson and P. N. Cheremisinoff). Marcel-Dekker, New York (1979).
6. H. Tabor, Nonconvecting solar ponds, *Phil. Trans. R. Soc. Lond.* **A295**, 423–433 (1980).
7. L. J. Wittenberg and D. E. Etter, Heat extraction from a large solar pond, ASME Paper No. 82-WA/SOL-31 (1982).
8. Y. Jaluria, Heat rejection and energy extraction within solar ponds, Solar Energy Research Institute, Golden, Colorado, Rep. SERI/RR-252-1393 (1982).
9. F. Zangrando, Heat and mass extraction from solar ponds: analysis and development of a laboratory facility, Solar Energy Research Institute, Colorado, Rep. SERI/RR-252-1569 (1982).
10. S. K. Gupta and Y. Jaluria, An experimental and analytical study of thermal stratification in an enclosed water region due to thermal energy discharge, *Energy Conversion* **22**, 63–70 (1982).
11. W. J. Wang and C. P. Lee, Dynamic response of solar heat storage systems, ASME Winter Annual Meeting, New York, ASME Paper No. 74-WA/HT-22 (1974).
12. Y. Jaluria, *Natural Convection Heat and Mass Transfer*, Chap. 2. Pergamon Press, Oxford (1980).
13. W. L. Oberkampf and L. I. Crow, Numerical study of the velocity and temperature fields in a flow through a reservoir, *Trans. Am. Soc. Mech. Engrs*, Series C, *J. Heat Transfer* **98**, 353–359 (1976).
14. S. V. Patankar, *Numerical Methods in Heat Transfer and Fluid Flow*, Chap. 6. Hemisphere, Washington, DC (1980).
15. Y. Jaluria and S. K. Gupta, A numerical study of mixed convection in enclosures, *Int. J. Energy Res.* **7**, 201–210 (1983).
16. D. W. Peaceman and H. H. Rachford, The numerical solution of parabolic and elliptic differential equations, *J. Soc. Ind. Appl. Math.* **3**, 28–41 (1955).
17. C. K. Cha, An analytical and numerical investigation of recirculating mixed convection flow in an enclosure, Ph.D. thesis, Rutgers University, New Brunswick, New Jersey (1983).
18. R. C. Y. Koh, Two-dimensional surface warm jets, *ASCE J. Hyd. Div.* **97**, 819–836 (1971).

ECOULEMENT DE CONVECTION MIXTE AVEC RECIRCULATION POUR L'EXTRACTION D'ENERGIE

Résumé—L'énergie stockée par chaleur sensible dans un corps peut être extraite par un fluide en écoulement avec recirculation. Une étude numérique de l'écoulement variable, bidimensionnel, laminaire est faite. Le fluide chaud est envoyé au sommet tandis que le fluide froid sort à la base de la région de stockage pour préserver la stratification thermique. La nature de l'écoulement est fortement affectée par les forces d'Archimède et la configuration de l'écoulement. Des résultats numériques sont présentés pour un large domaine de paramètres opératoires qui caractérisent les conditions d'entrée, la configuration de l'écoulement et les mécanismes de transfert thermique aux frontières.

REZIRKULIERENDE MISCHKONVEKTIONS-STRÖMUNGEN ZUR ENTZIEHUNG VON ENERGIE

Zusammenfassung—Energie, die als fühlbare Wärme in einer Flüssigkeit innerhalb eines Behälters gespeichert ist, kann mit Hilfe einer Rezirkulationsströmung entzogen werden. Eine rechnerische Untersuchung der auftretenden zeitabhängigen zweidimensionalen laminaren Konvektionsströmung wurde durchgeführt. Die heiße Flüssigkeit wird an der Oberseite des Speichers abgezogen und nach der Abkühlung an der Unterseite wieder zugeführt, um die thermische Schichtung aufrechtzuerhalten. Es zeigt sich, daß die Art der Strömung stark vom Auftrieb und der Strömungsform beeinflußt wird. Numerische Ergebnisse werden für einen weiten Bereich von Parametern vorgelegt, die von den Einströmbedingungen, der Strömungsform und den Wärmeübertragungsmechanismen an den Grenzen abhängen.

ИСПОЛЬЗОВАНИЕ РЕЦИРКУЛЯЦИОННЫХ ПОТОКОВ ПРИ СМЕШАННОЙ КОНВЕКЦИИ ДЛЯ ПОЛУЧЕНИЯ ТЕПЛОВОЙ ЭНЕРГИИ

Аннотация—С помощью рециркуляционного течения можно получить тепловую энергию за счет физической теплоты, содержащейся в объеме жидкости. Проведено численное исследование нестационарного двумерного ламинарного течения, возникающего в такой ситуации. Для поддержания тепловой стратификации нагретая жидкость отводится из верхней части резервуара, а охлажденная – из нижней. Показано, что характер течения сильно зависит от сил плавучести и структуры потока. Результаты расчетов представлены для широкого диапазона основных параметров, определяемых условиями на входе потока, его конфигурацией и механизмами теплопереноса на границах.